Hindawi
Advances in Polymer Technology
Volume 2022, Article ID 9968902, 13 pages
https://doi.org/10.1155/2022/9968902

Research Article

Fiber Orientation Analysis of Overflow Water-Assisted Injection Molding with Short Glass Fiber Reinforced Polypropylene

Dongyou Huang,[1,2] **Hesheng Liu**,[1,3] **Tangqing Kuang**,[3] **and Zhong Yu**[4]

[1]Polymer Processing Laboratory, Nanchang University, Nanchang 330031, China
[2]Jiaxing Management Center of Primary and Secondary School Teacher Training, Jiaxing Education Institute, Jiaxing 314051, China
[3]School of Mechanical & Electrical Engineering, East China Jiaotong University, Nanchang 330013, China
[4]Jiangxi Key Laboratory of Polymer Preparation and Processing of Shangrao Normal University, Shangrao 334001, China

Correspondence should be addressed to Hesheng Liu; hsliu@vip.163.com

Received 5 January 2022; Accepted 19 April 2022; Published 13 May 2022

Academic Editor: Xianglan Bai

The fiber orientation is playing an important performance indexed for glass fiber reinforced polypropylene for water-assisted injection molding. Based on the viscoelastic constitutive equation (White-Metzner) and the fiber orientation model (iARD-RPR), the effects of fiber mass content, water injection delay time, water injection pressure, and melt temperature, which are on the fiber orientation along the flow direction and shear rate distribution of the melt, were investigated. Studies found that the orientation degree of the fiber along the flow direction was reduced with the increase of the fiber mass content, the extension of the water injection delay time, and the improvement of the melt temperature and that the orientation degree of the fiber along the flow direction was raised with the increase of the water injection pressure flow in the laminar flow state, but it was reduced with the increase in the turbulent state. It can be further learned from the shear rate distribution that decreasing fiber mass content, reducing the water injection delay time, lower melt temperature, and increasing water injection pressure in laminar flow conditions will increase the shear rate in the channel layer and the shear rate gradient along the thickness direction of the melt, while the water injection pressure in the turbulent state is on the contrary.

1. Introduction

As a medium-assisted molding technology in injection molding, water-assisted injection molding (WAIM) is favored by insiders in the industry because of its advantages of saving raw materials, reducing the weight of parts, enhancing physical and mechanical properties, shortening the molding cycle, and so on [1, 2]. Gas-assisted injection molding (GAIM) has the same strength as WAIM. These two molding methods are collectively referred to as fluid-assisted injection molding, and the molding principles of them are the same. However, as to fluid media, water has higher thermal conductivity, specific heat capacity, and incompressibility than gas, which makes WAIM have shorter molding cycles, higher internal surface smoothness of molded parts, and more abundant size of molded part than GAIM [3, 4]. The WAIM can be classified into short-shot water-assisted injection molding (SWAIM) and overflow water-assisted injection molding (OWAIM) in the light of whether the polymer melt is filled in the main cavity before water injection.

Based on the two molding methods above, the researchers conducted macroscopic and microscopic properties research such as water penetration length, residual wall thickness, and crystal morphology according to process parameters, physical parameters, and mold structure parameters. In terms of macroscopic performance, Liu [5, 6] and Zhang [7] have studied the effects of relevant process parameters on the water penetration of water-assisted injection products. Huang et al. [8] studied the influence of process parameters on water penetration length and residual wall thickness of polypropylene (PP) elbow pipe products by the single factor method. Polynkin et al. [9] simulated the effect of water injection pressure on the residual wall thickness of water-assisted injection circular pipe products. Pudpong et al. [10] used Moldflow to simulate and analyze the influence of process parameters on the residual wall thickness of overflow water-assisted injection PP products. Liu [11] studied the effect of crystal morphology on water-assisted injection HDPE products based on different melt temperatures and different molecular weights.

Nowadays, on the basis of the broad prospects of PP and the excellent properties of glass fiber, such as good hygroscopicity, heat insulation, and shock resistance [12], the research on the injection molding of glass fiber reinforced polypropylene (GFPP) has attracted much attention. In terms of performance research, Tang Xiao et al. [13] pointed out that GFPP has excellent comprehensive properties such as stable size, good fatigue resistance, and small shrinkage; Scheme revealed that GFPP has good molding flowability and convenient processing [14]; Zhou et al. find that the length of the glass fiber has an obvious effect on the mechanical properties of the composite [15] and fiber orientation is essential for enhancing the mechanical properties of glass-fiber-reinforced polymer [16]. In terms of the molding mechanism, Liu [5] revealed that the fibers in the WAIM of short fiber reinforced PP are along the flow direction at the interface between the polymer and the mold wall as well as between the polymer and water; Huang et al. [17] studied the fiber orientation pattern of water-assisted injection fiber-reinforced polypropylene parts and explained its formation mechanism by using the unique shear rate and cooling rate fields of melt filling and high-pressure water penetration into the cavity; Wang [18] studied the effect of the formation mechanism of PP or acrylonitrile-styrene copolymer on the transverse crystal formation based on relevant process parameters and physical parameters. In terms of fiber orientation, Loekett [19] qualitatively predicts the law of fiber orientation due to the flow that in the case of convergent flow and shear flow, the fiber orientation tends to the flow direction, while in the case of divergent flow, it is perpendicular to the flow direction; Zhou [20] has made some progress in theoretical calculation and computer simulation of fiber orientation in short fiber filled plastics and obtained some schematic diagrams of fiber orientation distribution; Fisa et al. [21] used scanning electron microscopy to study the fusion line of glass fiber reinforced polypropylene injection mold and observed that in the plate model, the orientation of the fiber in the fusion line area was almost parallel to the flow direction. By improving the short-shot water-assisted injection molding process, Yu et al. [22] found that the water injection parameters affected the fiber orientation in the front half of the injection molding process of short-shot glass fiber-reinforced polypropylene.

The above research shows that the influence of flow behavior on fiber orientation is very complex, but at present, the prediction of fiber orientation is mostly from the qualitative point of view, and the research on fiber orientation control has not yet been proposed. On the premise of determining the material, the relationship between the injection molding process parameters and fiber orientation is comprehensively grasped, which is beneficial to optimize the injection molding process parameters and improve the fiber orientation in the fiber reinforced injection molded parts.

In this paper, the fiber orientation along the flow direction has been studied by changing the physical properties and process parameters, such as fiber content, melt temperature, water injection pressure, and water injection delay time.

2. Numerical Research Method

OWAIM method of short fiber reinforced polypropylene comprises the following steps: Firstly, fill the composite materials into the entire main cavity. Secondly, inject high-pressure water into the main cavity through the water injection nozzle to push the molten composite material to the overflow cavity. Finally, maintain pressure and cool down. Throughout the process, there are many factors affecting the orientation of the fibers along the flow direction, such as fiber content, melt temperature, mold temperature, water injection delay time, water injection pressure, water injection temperature, water pressure duration time and so on.

During the WAIM of short fiber-reinforced polymer composites, Liu [5, 6] experimentally studied the influence of process parameters on water penetration, but only revealed the characteristics of WAIM in fiber orientation (three-layer structure, including the mold wall layer, core layer, and water channel layer). According to the previous research results, this paper focuses on fiber mass content, melt temperature, water injection delay time, and water injection pressure to study the fiber orientation along the flow direction and determine its influence law.

3. Mathematical Models and Assumptions

OWAIM involves not only short fiber reinforced polypropylene composites with viscoelastic melts, but also high pressure water with Newtonian fluids. To converge the calculation and conform the actual molding conditions, the mathematical model has been simplified as follows:

(1) The density, heat capacity, and thermal conductivity of the fluid are kept unchanged

(2) There is no slip phenomenon between the melt and the mold wall

(3) The surface tension, gravity, inertial force, and body force were ignored

(4) The enthalpy of phase transition in the process of melt crystallization is not considered

Therefore, the governing equations for obtaining three-dimensional non-isothermal flow behavior are as follows:

Continuity equation:

$$\frac{\partial \rho}{\partial t} + \nabla \cdot \rho \boldsymbol{u} = 0, \tag{1}$$

Table 1: Characteristics of polypropylene-based short fiber composites.

Characteristic parameter	Fiber mass content 10%	20%	30%
Melt flow rate, (230 °C/2.16 kg)	7.0 g/10 min	6.0 g/10 min	5.0 g/10 min
Density, (23 °C)	0.96 g/cm^3	1.03 g/cm^3	1.12 g/cm^3
Flexural modulus	2000 MPa	3300 MPa	4700 MPa
Tensile stress at yield	38.0 MPa	50.0 MPa	61.0 MPa
Notched Izod impact strength, (23 °C)	11 kJ/m^2	14 kJ/m^2	18 kJ/m^2
Thermal conductivity	$k = 0.1776$W/(m.K)	$k = 0.2$W/(m.K)	$k = 0.2$W/(m.K)
Specific heat capacity	$C_P = 2700$J/(kg.K)	$C_P = 3100$J/(kg.K)	$C_P = 3100$J/(kg.K)
White-Metzner constitutive equation parameters	$n = 0.20426$, $\tau^* = 33086.7$Pa, $D_1 = 4.58E + 20$Pa · s, $D_2 = 263.15$K, $D_3 = 0$K/Pa, $A_1 = 40.388$, $\tilde{A}_2 = 51.6$K, G = 2.1E + 05Pa	$n = 0.212208$, $\tau^* = 55735.9$Pa, $D_1 = 1.35E + 17$Pa · s, $D_2 = 273.15$K, $D_3 = 0$K/Pa, $A_1 = 33.2285$, $\tilde{A}_2 = 51.6$K, G = 1.0E + 05Pa	$n = 0.254166$, $\tau^* = 40081.3$Pa, $D_1 = 6.46E + 27$Pa · s, $D_2 = 273.15$K, $D_3 = 0$K/Pa, $A_1 = 55.7621$, $\tilde{A}_2 = 51.6$K, G = 1.2E + 05Pa
Fiber orientation model iARD-PRP parameters		$C_I = 0.005, C_M = 0, \alpha = 0.7$	

Momentum equation:

$$\frac{\partial}{\partial t}(\rho \boldsymbol{u}) + \nabla \cdot (\rho \boldsymbol{u}\boldsymbol{u} + \boldsymbol{\tau}) = -\nabla p + \rho \boldsymbol{g}, \quad (2)$$

Energy equation:

$$\rho C_p\left(\frac{\partial T}{\partial t} + \boldsymbol{u} \cdot \nabla T\right) = \nabla \cdot (k\nabla T) + \eta\dot{\gamma}^2, \quad (3)$$

Where $\boldsymbol{u}$ = velocity vector, T = temperature, t = time, p = pressure, $\boldsymbol{\tau}$ = stress tensor, $\boldsymbol{g}$ = acceleration vector of gravity, ρ = density, η = viscosity, k = thermal conductivity, C_p = specific heat and $\dot{\gamma}$ = shear rate.

To describe the rheological properties of the polymer melt in the mold flow channel, one of the classical constitutive equations reflecting the short fiber-reinforced polymer composites, the White-Metzner constitutive equation, is selected:

$$\begin{aligned}
&\boldsymbol{\tau} + \lambda\left(\frac{\partial \boldsymbol{\tau}}{\partial t} + \boldsymbol{u} \cdot \nabla\boldsymbol{\tau} - \nabla\boldsymbol{u}^{\mathrm{T}} \cdot \boldsymbol{\tau} - \boldsymbol{\tau} \cdot \nabla\boldsymbol{u}\right) = \eta\left(\nabla\boldsymbol{u} + \nabla\boldsymbol{u}^{\mathrm{T}}\right),\\
&\lambda(T, \dot{\gamma}) = \frac{\eta(T, \dot{\gamma})}{G},\\
&\eta = \frac{\eta_0}{1 + (\eta_0\dot{\gamma}/\tau^*)^{1-n}},\\
&\eta_0 = D_1 \exp\left(\frac{-A_1(T - T_c)}{A_2 + (T - T_c)}\right),\\
&T_c = D_2 + D_3 p,\\
&A_2 = \tilde{A}_2 + D_3 p,
\end{aligned} \quad (4)$$

where T = melt temperature, G = shear modulus; η_0 = zero shear viscosity; τ^* = the parameter of the transition region between zero shear rate and the power law region of the viscosity curve; n = the power law index; and D_1, D_2, D_3, A_1, and $\tilde{A}_2$ are the material constants.

To reflect the fiber orientation of short fiber-reinforced polypropylene composites in injection molding, the orientation model iARD-RPR was selected [23], and the equations are as follows:

$$\begin{aligned}
&\dot{\mathbf{A}} = \dot{\mathbf{A}}^{\mathrm{HD}} + \dot{\mathbf{A}}^{\mathrm{iARD}}(C_I, C_M) + \dot{\mathbf{A}}^{\mathrm{RPR}}(\alpha),\\
&\dot{\mathbf{A}}^{\mathrm{HD}} = (\mathbf{W} \cdot \mathbf{A} \text{-} \mathbf{A} \cdot \mathbf{W}) + \xi(\mathbf{D} \cdot \mathbf{A} + \mathbf{A} \cdot \mathbf{D} \text{-} 2\mathbf{A}_4 : \mathbf{D}),
\end{aligned} \quad (5)$$

where $\dot{\mathbf{A}}^{\mathrm{iARD}}$ has two available parameters: the fiber-fiber interaction parameter C_I and the fiber-matrix interaction parameter C_M; and $\dot{\mathbf{A}}^{\mathrm{iARD}}$ has one parameter α, which is meant to slow down the response rate of the fiber orientation.

In this paper, the material selected three kinds of polypropylene composites with a mass content of 10%, 20%, and 30% short fibers, which were produced by LyondellBasell Industries. According to the equations mentioned above, the physical parameters involved are shown in Table 1.

3.1. Melt Front Tracking. A volume percent function is introduced to describe the melt front position and the evolution of fluid penetration with respect to time. $f = 0$ is defined as the fluid phase, $f = 1$ is defined as the plastic melt phase, whereas the melt front is located in the $0 < f < 1$ cell. The increase in volume percent fraction of the kinematics process is governed by the following advection equation:

$$\frac{\partial f}{\partial t} + \nabla \cdot (\boldsymbol{u} f) = 0, \quad (6)$$

where f is the volume percent fraction and $\boldsymbol{u}$ is the velocity vector.

In this paper, based on the White-Metzner constitutive equation describing the short fiber reinforced polymer

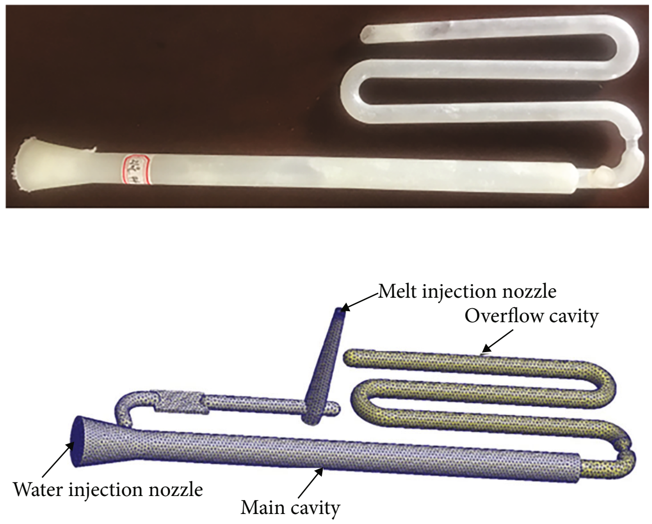

Figure 1: overflow water-assisted injection model.

Table 2: The process parameters.

Water injection delay time (s)	Water injection pressure (MPa)	Melt temperature (°C)
0	4	210
1	6	**230**
3	**8**	250
5	10	270

Note: The bold fonts in the table are the basic parameters to investigate melt temperature, water injection delay time, and water injection pressure.

composite and the short fiber orientation model iARD-PRP, a mathematical model was constructed based on the three major equations of fluid dynamics.

3.2. Model Structure and Process Parameters. The overflow water-assisted injection model structure mainly consists of a main cavity, an overflow cavity, a melt injection nozzle, and a water injection nozzle. Its main structural parameters are as follows: the main cavity size is $\Phi 16*245$, and the overflow cavity diameter is $\Phi 10$, as is shown in Figure 1.

In this paper, we have investigated the effects of fiber mass content, melt temperature, water injection delay time, and water injection pressure on the fiber orientation of overflow water-assisted injection molding of short fiber reinforced polypropylene composite. Here are the results of the process parameters in Table 2.

4. Results and Analysis

To understand the fiber orientation of short fiber reinforced PP in the process of OWAIM, the system has chosen the polypropylene matrix composite with 10% fiber mass content at 230 °C, water injection pressure 8 MPa, and water injection delay time 1 s. The fiber orientation along the flow direction as a function of injection time is shown in Figure 2.

It can also be seen from the figure that the melt is injected into the cavity from the injection nozzle to the entire main cavity (Figures 2(a)–2(c)) and the fiber orientation near the mold wall is higher than the middle of the flow channel, which is mainly due to the rapid cooling and solidification of the high-temperature melt when it meets the low-temperature mold wall, and the other end is subjected to shear action of the melt flow. The high-pressure water is injected from the water injection nozzle of main cavity, pushing the melt to the overflow cavity (Figures 2(d)–2(f)). The fiber of high orientation degree at the water channel along the flow direction further promotes the fiber orientation at the mold wall; the main reason is that the injection of high-pressure water promotes the solidification of the melt at the water channel and drives one end of the fiber to be oriented along the flow direction, simultaneously driving the shearing action along the thickness direction, thereby promoting the overall orientation of the fiber along the thickness direction. In order to gain a deeper understanding of the effect of the physical properties and process parameters on the orientation of the fibers along the flow direction, the shear rate distribution caused by high pressure water injection into the melt was introduced, and the fiber mass content, water injection delay time, water injection pressure, and melt temperature were discussed.

5. Effect of Fiber Mass Content

Figures 3 and 4 show how the polypropylene -based composites with different fiber mass contents behave in terms of the distribution of fiber orientation along the flow direction, and the shear rate distribution (melt temperature 230 °C, the water injection pressure is 8 MPa, and the water injection delay time is 1 s).

It can be seen from Figure 3 that the fiber orientation is the highest when the fiber mass content is 10%, followed by the fiber mass content of 20%, and finally the fiber mass content is 30%. The main reason is that when the fiber content is

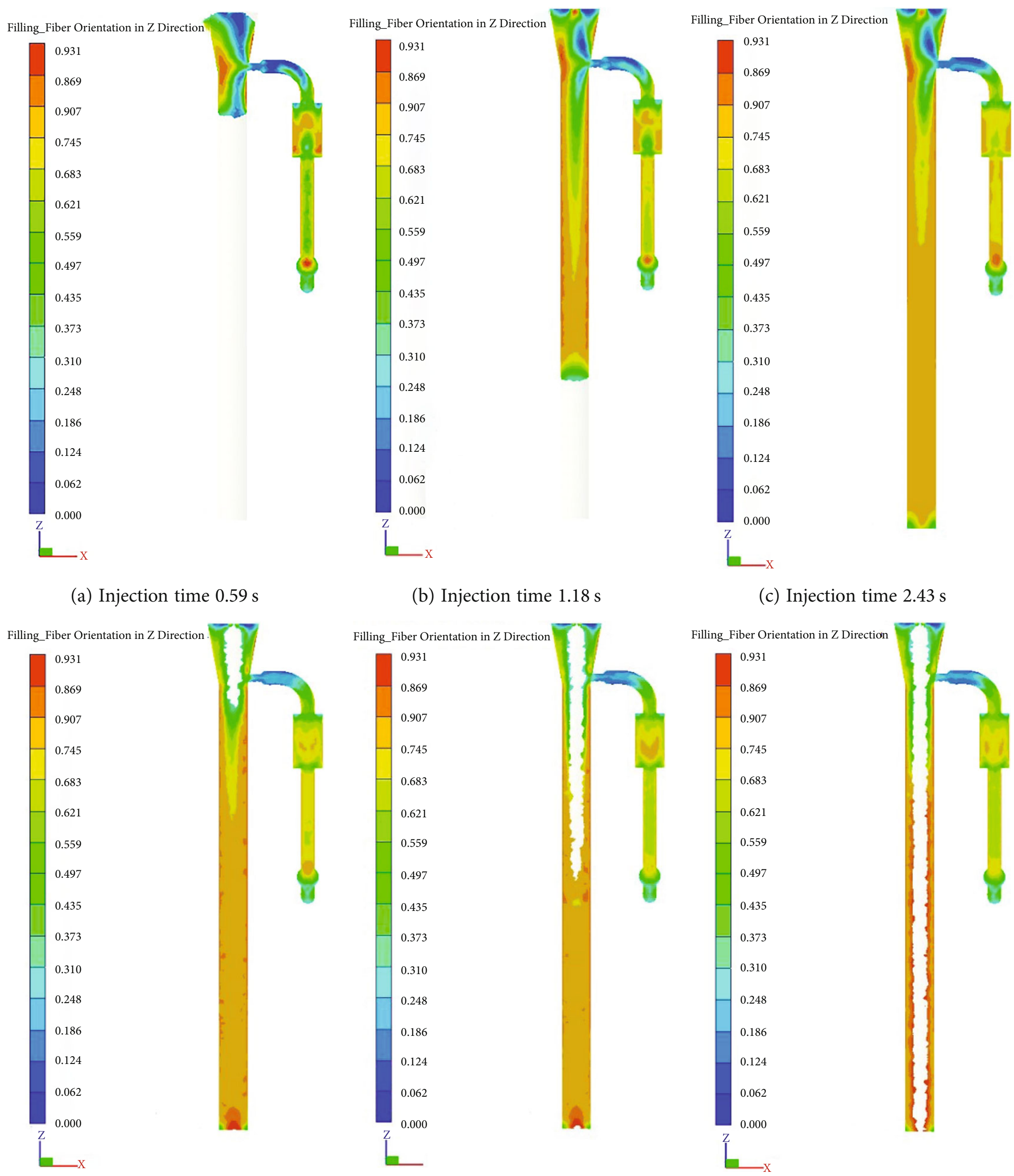

(a) Injection time 0.59 s
(b) Injection time 1.18 s
(c) Injection time 2.43 s
(d) Injection time 3.57 s
(e) Injection time 4.76 s
(f) Injection time 7.5 s

Figure 2: Distribution of fiber orientation along the flow direction in water-assisted injection molding of PP-based composites with 10% fiber mass content.

low, the interference between fibers is less under the action of strong shear, and it is easier to shear orientation; with the increase of fiber content, the fiber density is also increasing, the degree of mutual interference between fibers is increasing, and the resistance of shear orientation is greater, so the fibers are more likely to break under the action of strong shear, and the degree of fiber orientation is lower.

The shear rate gradient distribution is shown in Figure 4: The highest shear rate gradient as the fiber mass content is 10%, followed by the fiber mass content of 20%, and finally the fiber mass content of 30%. Driven by the injection of high-pressure water, the shear rate gradient of the melt is distributed along the thickness direction (from the water channel layer to the mold wall layer). The shear rate gradient is affected by shear stress and viscosity. Because of the same water injection pressure and the fact that water is a Newtonian fluid, the melts of different fiber mass contents are subjected to the same shear stress in the water channel. The viscosity is affected by the thermal conductivity and the rheological property constant. With the decrease of fiber content, the viscosity of the melt began to decrease, and the viscosity of the polypropylene

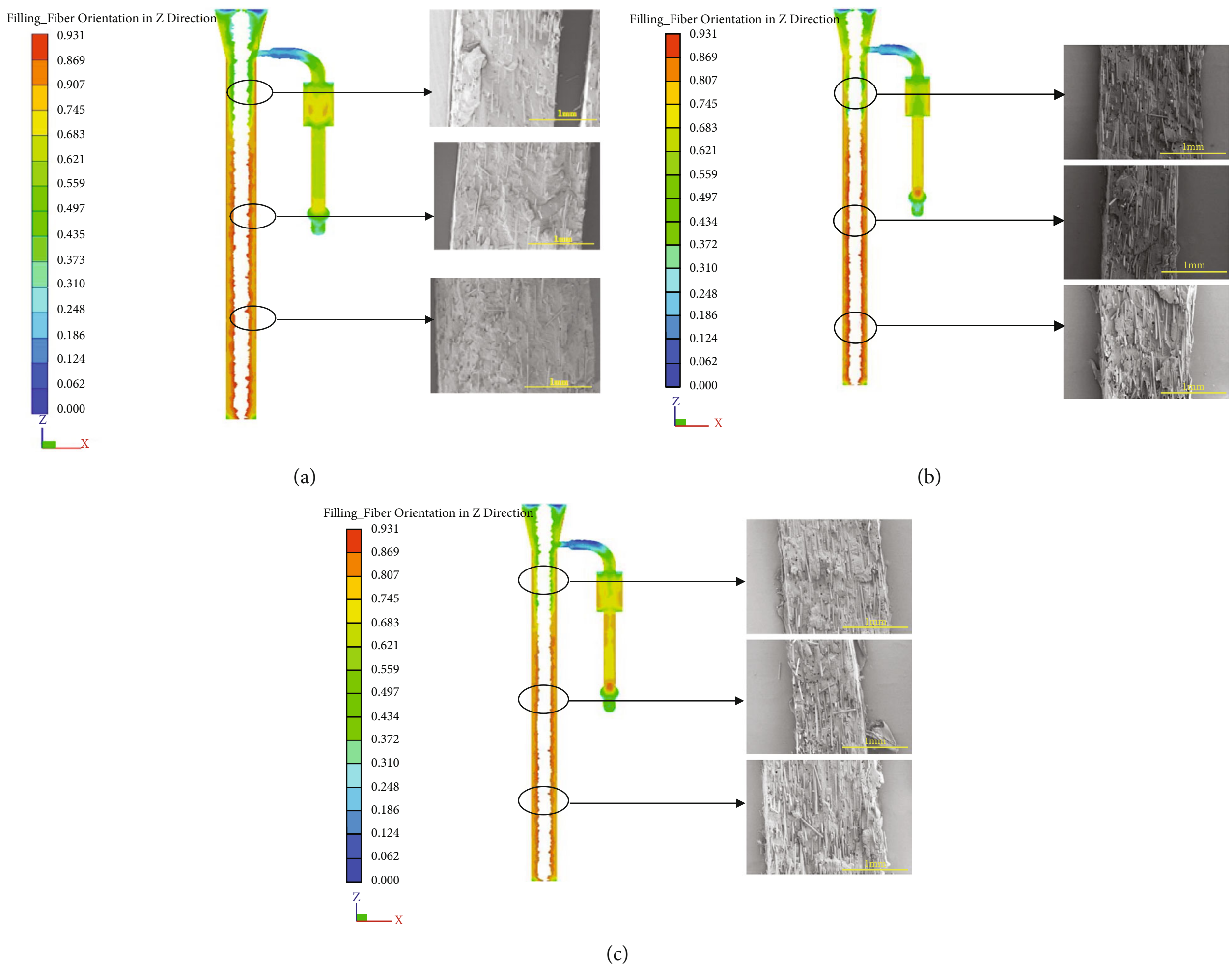

Figure 3: Fiber orientation distribution of different fiber mass content along the flow direction.

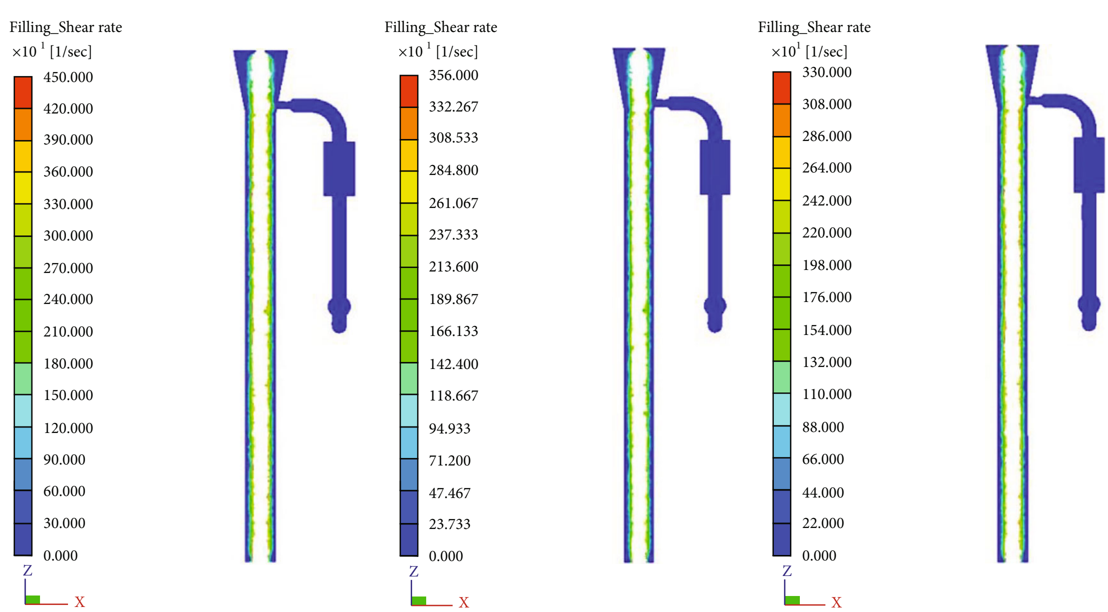

(a) GF10% (b) GF20% (c) GF30%

Figure 4: Shear rate distribution of different fiber mass content.

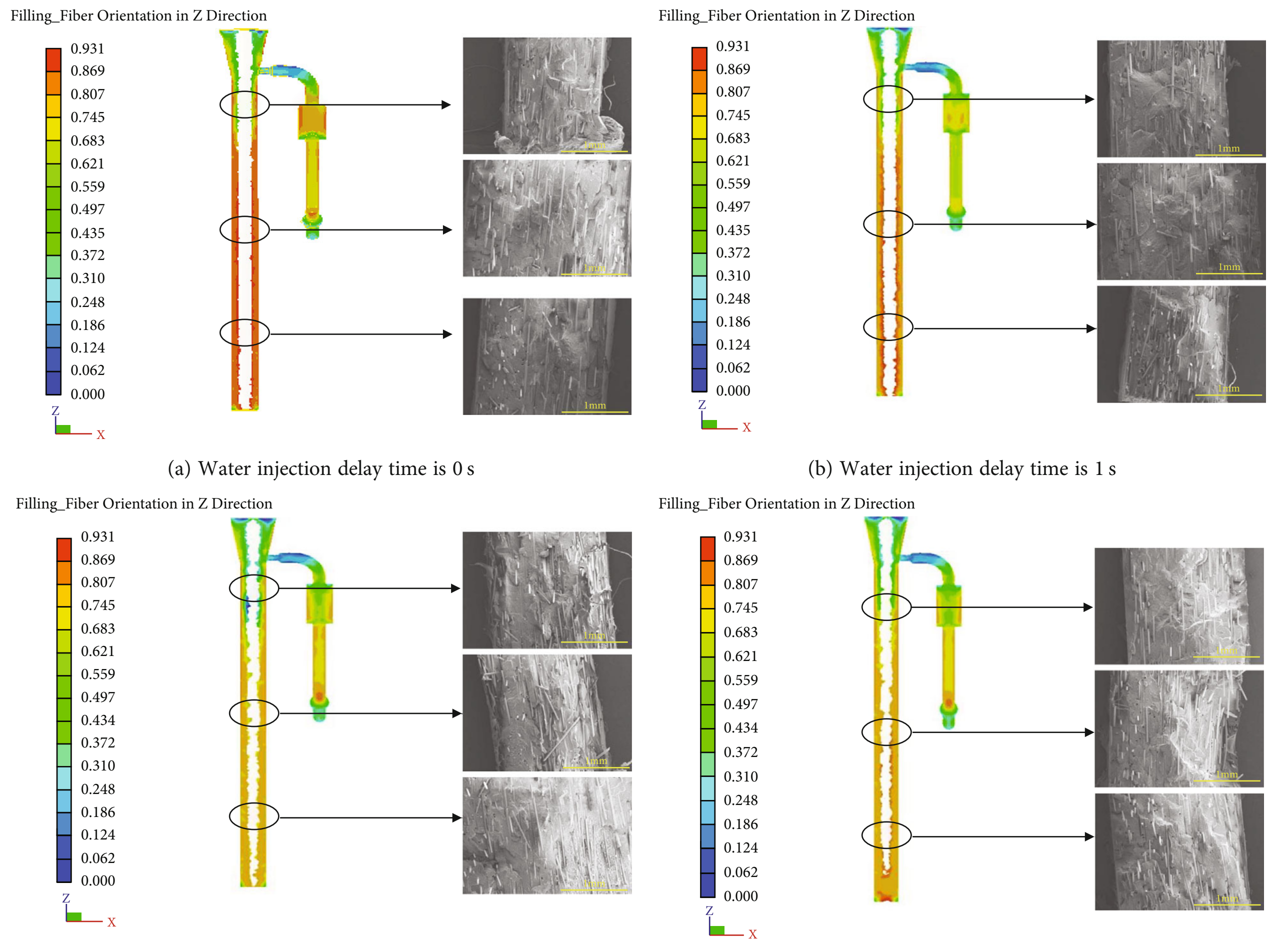

(a) Water injection delay time is 0 s

(b) Water injection delay time is 1 s

(c) Water injection delay time is 3 s

(d) Water injection delay time is 5 s

Figure 5: Fiber orientation distribution along the flow direction at different water injection delay time.

composite with 10% fiber content was the lowest, and its shear rate and gradient were the highest under the same high pressure water. When the fiber content is less, the internal friction between fibers in the melt is relatively small, the interference between fibers is not strong, and the higher the shear rate is, the higher the degree of fiber orientation is. Therefore, the fiber orientation is the highest when the fiber content is 10%.

6. Effect of Water Injection Delay Time

Figures 5 and 6, respectively, show the fiber orientation distribution along the flow direction and the shear rate distribution of polypropylene-based composites with 10% fiber mass content when the water injection delay time is 0 s, 1 s, 3 s, and 5 s; the melt temperature is 230°C; and the water injection pressure is 8 MPa.

It can be seen from Figure 5 that when the water injection delay time is 0 s, the fiber orientation is the highest, followed by 1 s water injection delay time and 3 s water injection delay time, and finally 5 s water injection delay time. The reason is mainly due to the extension of water injection delay time, which leads to better effect on the low temperature mold wall on the solidification of the melt, and the thickness of the solidification becomes thicker so that the viscosity increases in the whole thickness direction and the shear rate size distribution and the shear rate gradient field are smaller under the same shear stress.

As shown in Figure 6, the highest shear rate gradient at the water injection delay time is 0 s, followed by 1 s water injection delay time and 3 s water injection delay time, and finally 5 s water injection delay time.

7. Effect of Water Injection Pressure

Figures 7 and 8, respectively, show the fiber orientation distribution along the flow direction and the shear rate distribution of polypropylene-based composites with the 10% fiber mass content when the water injection pressure is 4 MPa, 6 MPa, 8 MPa, and 10 MPa, the delay time is 1 s, and the melt temperature is 230°C. It can be seen from Figure 7 that the highest fiber orientation is at 8 MPa water injection pressure, followed by 10 MPa water injection pressure and 6 MPa water injection pressure, and finally 4 MPa water injection pressure, which only causes the melt near the water end that is extruded to form a certain fiber

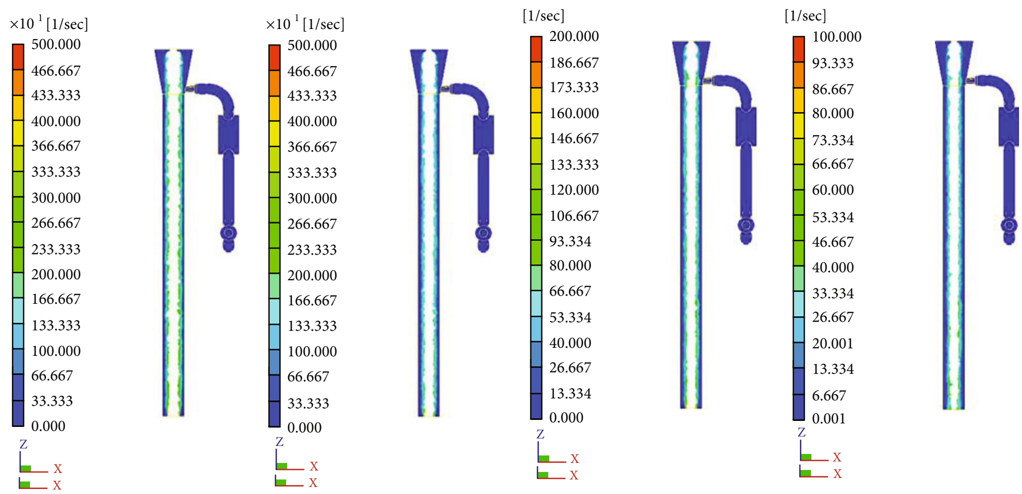

(a) (b) (c) (d)

Figure 6: Shear rate distribution at different water injection delay time.

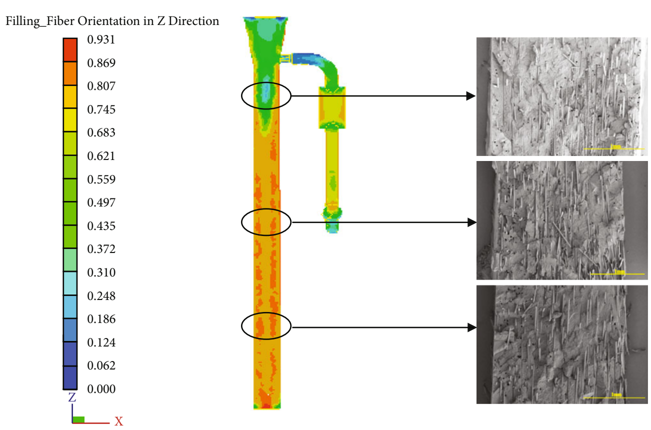

(a) Water injection pressure is 4 MPa

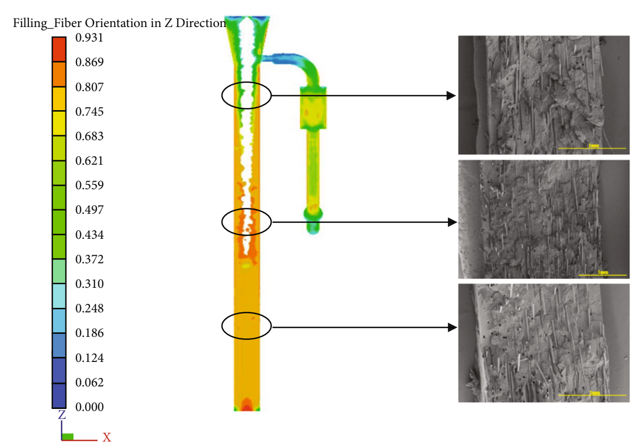

(b) Water injection pressure is 6 MPa

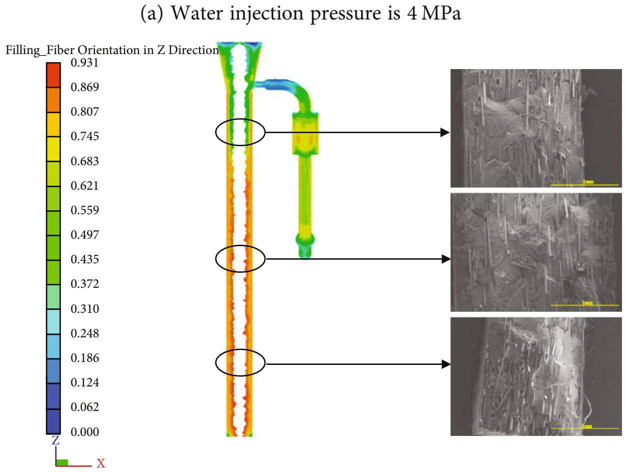

(c) Water injection pressure is 8 MPa

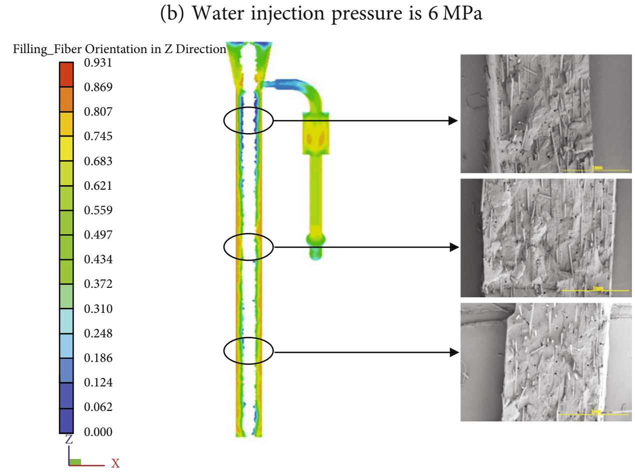

(d) Water injection pressure is 10 MPa

Figure 7: Fiber orientation distribution along the flow direction at different water injection pressure.

orientation, but the high-pressure water cannot penetrate the melt. The main reason is that with the increase of the water injection pressure, the water flow state changes from the original laminar flow to the turbulent flow, causing the fiber to change from ordered shear to disordered shear in the thickness direction, for example, when the water injection pressure

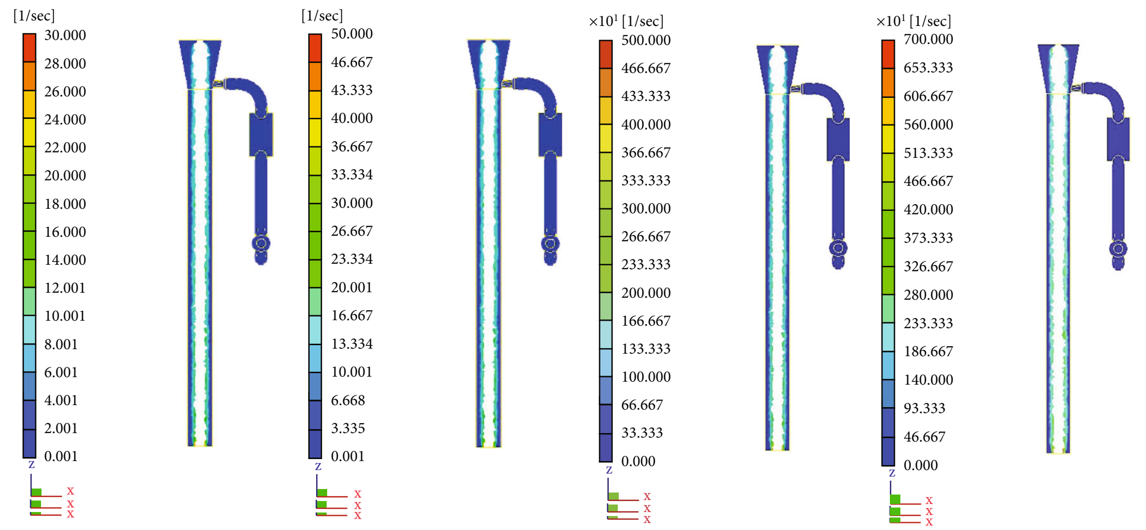

(a) 4 MPa (b) 6 MPa (c) 8 MPa (d) 10 MPa

Figure 8: Shear rate distribution at different water injection pressure.

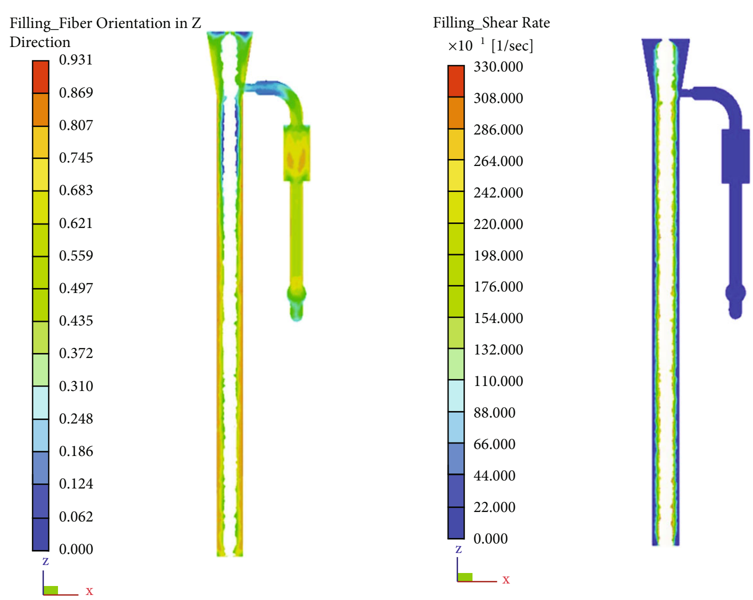

(a) Fiber orientation distribution along the flow direction (b) Shear rate distribution

Figure 9: Distribution of fiber orientation and melt shear rate at a water injection pressure of 9 MPa.

increases from 6 MPa to 8 MPa, the water flow state is laminar; but when the water injection pressure increases from 8 MPa to 10 MPa, the water flow state becomes turbulent. Therefore, the increase of water injection pressure causes the shearing action on the melt from increasing to decrease.

The shear rate distribution is shown in Figure 8: The highest shear rate gradient at water injection pressure is 8 MPa, followed by the water injection pressure of 10 MPa and the water injection pressure of 6 MPa, and finally the water injection pressure is 4 MPa.

To further verify that the fiber orientation distribution along the flow direction and the shear rate size distribution will decrease when the water injection pressure increases from 8 MPa to 10 MPa, the calculation result at 9 MPa is shown in Figure 9. As can be seen from Figures 8(b), 8(c), and 9, the previous analysis is reasonable.

8. Effect of Melt Temperature

Figures 10 and 11, respectively, show the fiber orientation distribution along the flow direction and the shear rate distribution of polypropylene-based composites with the 10% fiber mass content when the melt temperature is 210 °C, 230 °C, 250 °C, and 270 °C; the water injection pressure is 8 MPa; and the delay time is 1 s. It can be seen from Figure 10 that the highest fiber orientation is at the melt temperature of 210 °C, followed by the melt temperature of 230 °C and the melt temperature of 250 °C, and finally the

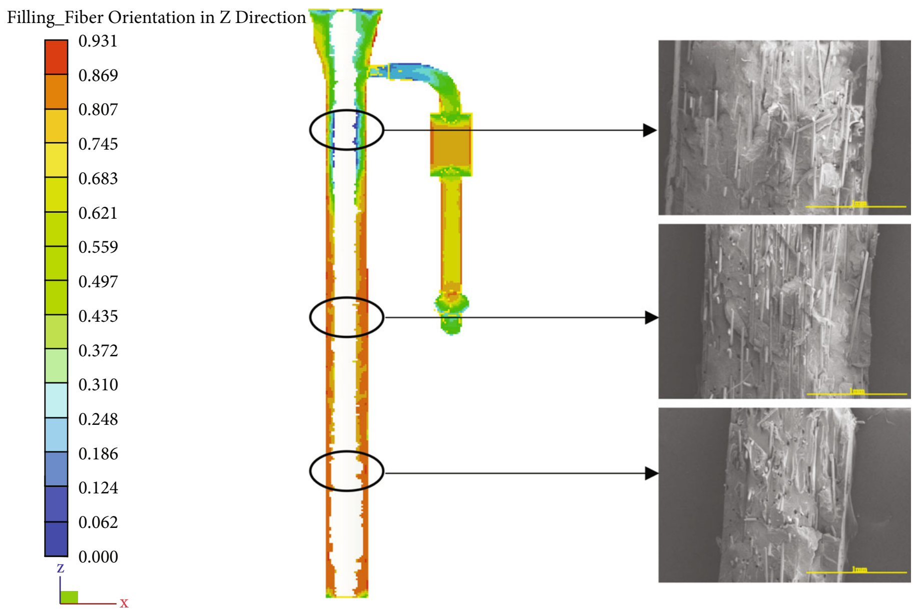

(a) Melt temperature is 210 °C

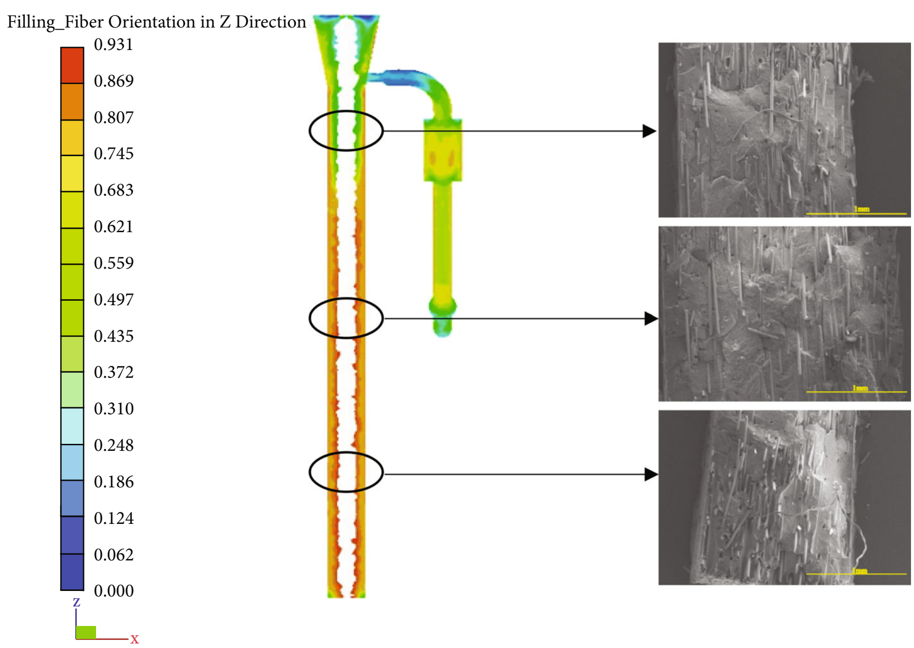

(b) Melt temperature is 230 °C

Figure 10: Continued.

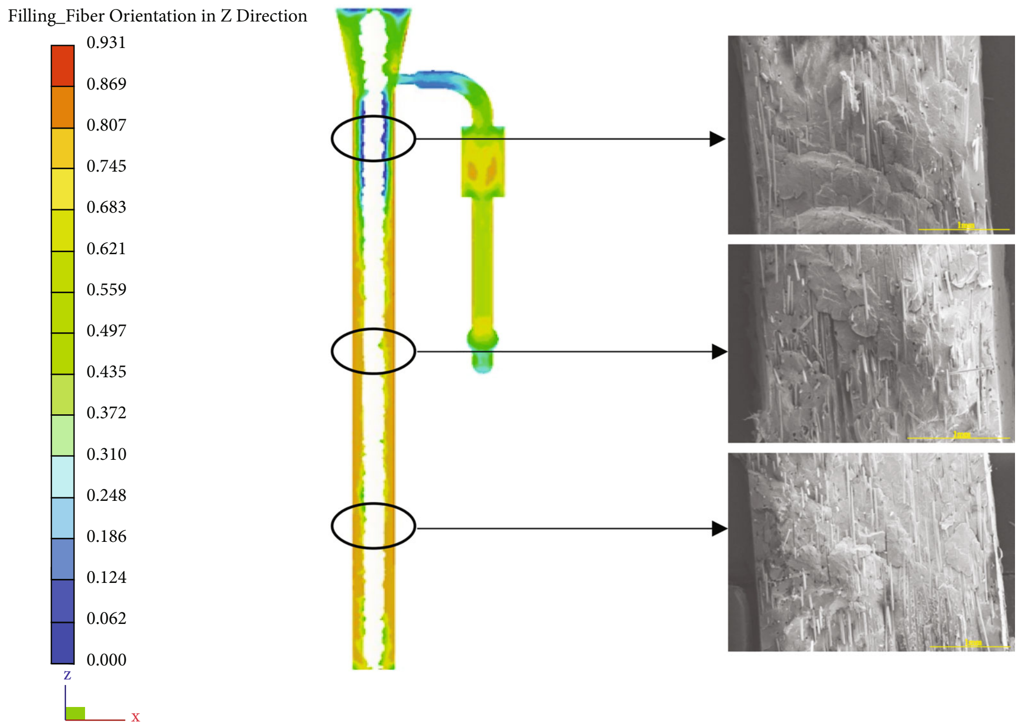

(c) Melt temperature is 250 °C

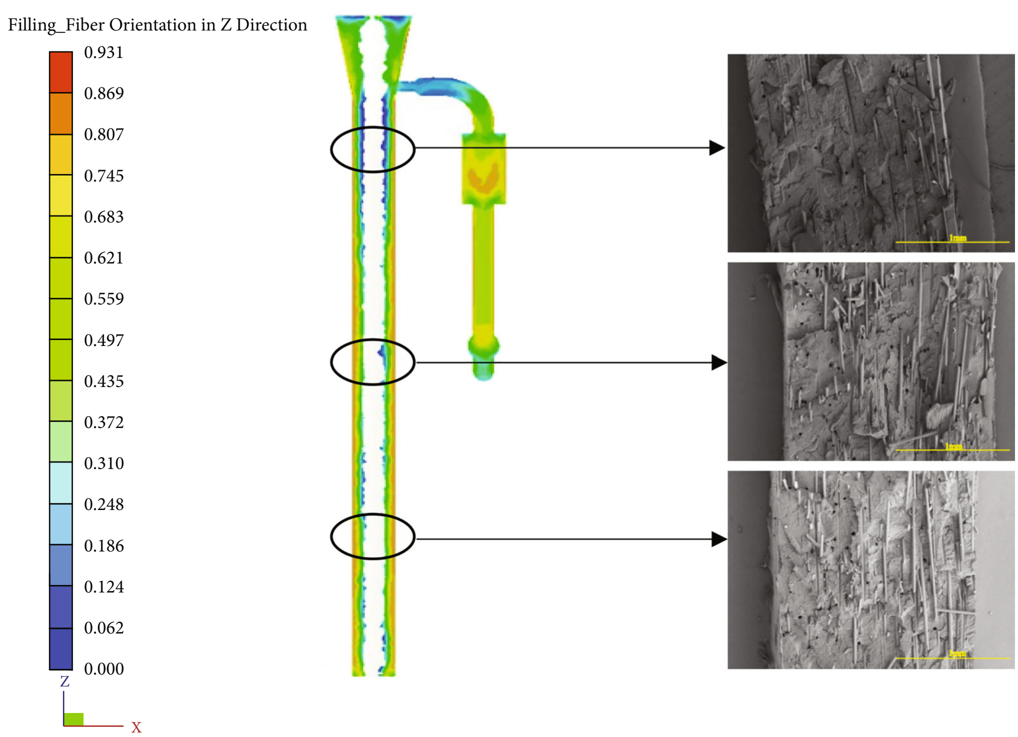

(d) Melt temperature is 270 °C

Figure 10: Fiber orientation distribution along the flow direction at different melt temperature.

melt temperature of 270 °C. The main reason is that as the melt temperature climbs higher, the melt viscosity decreases faster under the cooling effect of the low temperature mold wall and high pressure water, resulting in lower final viscosity of the high temperature melt.

Under the same shear stress, the melt of lower temperature has a larger shear rate size distribution and wider shear rate gradientl the shear rate distribution is shown in Figure 11: The highest shear rate gradient is at the melt temperature of 230 °C, followed by the melt temperature of

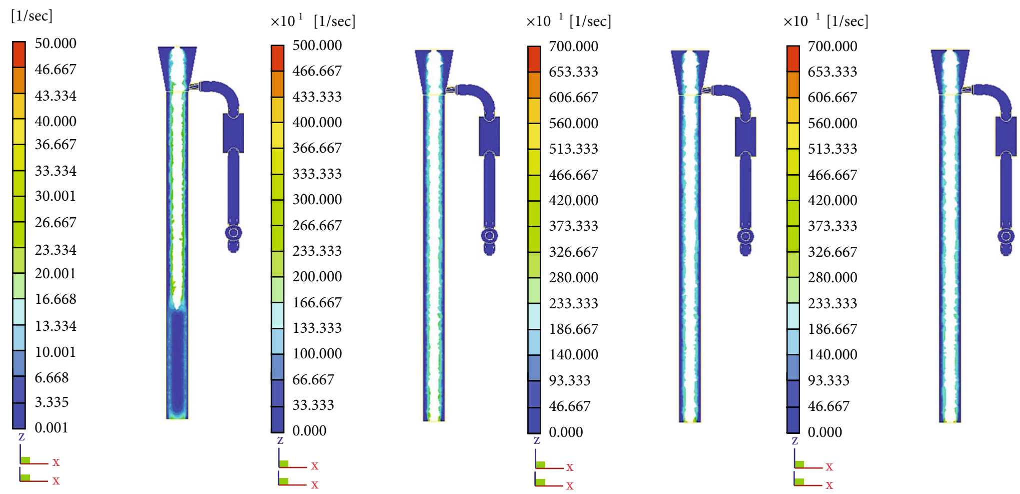

(a) 210 °C (b) 230 °C (c) 250 °C (d) 270 °C

Figure 11: Shear rate distribution at different melt temperature.

270 °C and 250 °C, and finally the melt temperature of 210 °C.

9. Conclusion

This essay does the analysis based on the combination of the viscoelastic constitutive equation White-Metzner of polypropylene-based short fiber composites and the fiber orientation model iARD-RPR. The effects of fiber mass content, water injection delay time, water injection pressure, and melt temperature on the orientation distribution of fibers along the flow direction of the main cavity section were analyzed. The results show that during the water-assisted injection molding process, the orientation of the fibers in the main cavity along the flow direction is higher at the mold wall layer and simultaneously lower at the center of the flow channel before the high-pressure water is injected; the orientation of the fibers in the main cavity along the flow direction at the water channel layer and the mold wall layer are higher after the high-pressure water injection, and the one at the core layer (between the water channel layer and the mold wall layer) is lower. In the main cavity, the orientation of the fibers along the flow direction will decrease with the increase of the fiber mass content, of water injection delay time increase, and of the melt temperature; as the water injection pressure increases to a certain extent (6 MPa to 8 MPa), the orientation of the fiber along the flow direction increases; however, as the water injection pressure continues to increase (8 MPa to 10 MPa), the orientation of the fibers along the flow direction decreases, which is mainly related to the flow state of the high-pressure water during the penetration process. In order to further realize the influence of these physical properties and process parameters on the orientation of the fibers along the flow direction, this paper analyzes the shear rate distribution of the melt after the injection of high-pressure water, which further confirming the influence of these parameters on the fiber orientation along the flow direction.

Data Availability

The data used to support the findings of this study are included with the article. Additional data can be made available upon reasonable request from the author.

Conflicts of Interest

The authors declare that they have no conflict of interest.

Acknowledgments

This work forms part of a project supported by the National Natural Science Foundation of China (NSFC, No. 21664002, No. 51563010, and No. 52163006), the Industrial Field of Science and Technology Department of Jiangxi Province (No. 20203BBE53065) and the Natural Science Foundation of Jiangxi Province (No. 2018BAB206014).

References

[1] M. Knights, "Water injection molding makes hollow parts faster," *Plastics Technology*, vol. 48, no. 4, pp. 42–47, 2002.

[2] T. Juntgen and W. Michaeli, *The water injection technique (WIT) as an attractive alternative and supplement to gas-assisted injection molding (GAIM)*, ANTEC 2002-Conference Proceedings, 2002.

[3] S. J. Liu and Y. S. Chen, "Water-assisted injection molding of thermoplastic materials: effects of processing parameters," *Polymer Engineering and Science*, vol. 43, no. 11, pp. 1806–1817, 2003.

[4] S. J. Liu and W. K. Chen, "Experimental investigation and numerical simulation of cooling process in water assisted injection moulded parts," *Plastics, Rubber and Composites*, vol. 33, no. 6, pp. 260–266, 2004.

[5] S. J. Liu and Y. S. Chen, "The manufacturing of thermoplastic composite parts by water-assisted injection-molding technology," *Composites Part A: Applied Science and Manufacturing*, vol. 35, no. 2, pp. 171–180, 2004.

[6] S.-J. Liu, M.-J. Lin, and W. Yi-Chuan, “An experimental study of the water-assisted injection molding of glass fiber filled poly-butylene-terephthalate (PBT) composites,” *Composites Science and Technology*, vol. 67, no. 7-8, pp. 1415–1424, 2007.

[7] Z. Zhang, H. Zhou, Y. Gao, and H. Yang, “Simulation and analysis on cavity filling process in water-assisted injection molding,” *Journal of Mechanical Engineering*, vol. 46, no. 8, pp. 140–146, 2010.

[8] H. X. Huang and Z. W. Deng, “Effects and optimization of processing parameters in water-assisted injection molding,” *Journal of Applied Polymer Science*, vol. 108, no. 1, pp. 228–235, 2008.

[9] A. Polynkin, L. Bai, J. F. T. Pittman et al., “Water assisted injection moulding: development of insights and predictive capabilities through experiments on instrumented process in parallel with computer simulations,” *Plastics, Rubber and Composites*, vol. 37, no. 2-4, pp. 131–141, 2008.

[10] T. Pudpong, P. Buahom, S. Areerat, W. Rungseesantivanon, I. Satoh, and T. Saito, “The effects of processing parameters on the residual wall thickness distribution at the sharp angle corner of water assisted injection molded parts,” *International Polymer Processing*, vol. 28, no. 5, pp. 528–540, 2013.

[11] X. Liu, C. Zhang, K. Dai, G. Zheng, C. Liu, and C. Shen, “Unexpected molecular weight dependence of shish kebab in water-assisted injection molded HDPE,” *Polymers for Advanced Technologies*, vol. 24, no. 2, pp. 270–272, 2013.

[12] Z. M. Luo, J. Deng, T. Wang, Y. Yang, X. Q. Wang, and F. Lin, “Research progress on preparation technology and properties of glass fiber thin-walled circular tube composite structure,” *CHINA PLASTICS INDUSTRY*, vol. 1, pp. 20–25, 2022.

[13] X. Tang, X. Y. Sun, and Z. W. Wang, “Glass fiber reinforced polypropylene composite: a review of lightweight material,” *Shanghai Plastics*, vol. 4, pp. 17–22, 2021.

[14] M. Schemme, “LFT - development status and perspectives,” *Plastics, Additives and Compounding*, vol. 10, no. 2, pp. 38–43, 2008.

[15] Y.-G. Zhou, S. Bei, and L.-S. Turng, “Mechanical properties, fiber orientation, and length distribution of glass fiber-reinforced polypropylene parts: influence of water-foaming technology,” *Polymer Composites*, vol. 39, no. 12, pp. 4386–4399, 2018.

[16] S. Bei and Y.-G. Zhou, “Influence of foaming technology on fibre breakage in long fibre-reinforced polypropylene composites parts,” *Plastics, Rubber and Composites*, vol. 46, no. 8, pp. 365–374, 2017.

[17] H. X. Huang, R. H. Zhou, and C. Yang, “Fiber orientation propelled by high-pressure water penetration in water-assisted injection molded fiber-reinforced thermoplastics part,” *Journal of Composite Materials*, vol. 47, no. 2, pp. 183–190, 2013.

[18] B. Wang, H.-x. Huang, and Z.-y. Wang, “Formation mechanism of transcrystals in PP/SAN blends prepared via water-assisted injection MOLDING,” *POLYMERICA SINICA*, vol. 12, no. 8, pp. 825–830, 2012.

[19] F. J. Loekett, “Prediction of fiber orientation in molded components,” *Plast Rubber Process*, vol. 6, pp. 85–94, 1980.

[20] Z. Chixing, “Modeling and simulation of flow process in low volume fraction with short fiber filled polymeric viscous fluids,” *Polymeric Materials Science and Engineering*, vol. 1, pp. 36–43, 1988.

[21] B. Fisa and M. Rahmani, “Weldline strength in injection molded glass fiber-reinforced polypropylene,” *Polymer Engineering and Science*, vol. 31, no. 18, pp. 1330–1336, 1991.

[22] Y. Zhong, H.-S. Liu, T.-Q. Kuang et al., “Numerical simulation during short-shot water-assisted injection molding based on the overflow cavity for short-glass fiber-reinforced polypropylene,” *Advances in Polymer Technology*, vol. 2020, 13 pages, 2020.

[23] H.-C. Tseng, R.-Y. Chang, and C.-H. Hsu, “Phenomenological improvements to predictive models of fiber orientation in concentrated suspensions,” *Journal of Rheology*, vol. 57, no. 6, pp. 1597–1631, 2013.